

# Errors in Heat Flux Measurement by Flux Plates of Contrasting Design and Thermal Conductivity

T. J. Sauer,\* D. W. Meek, T. E. Ochsner, A. R. Harris, and R. Horton

## ABSTRACT

The thermal conductivity ( $\lambda$ ) of soils may vary by a factor of about 4 for a range of field soil water contents. Measurement of soil heat flux ( $G$ ) using a heat flux plate with a fixed  $\lambda$  distorts heat flow through the plates and in the adjacent soil. The objectives of this research were to quantify heat flow distortion errors for soil heat flux plates of widely contrasting designs and to evaluate the accuracy of a previously reported correction. Six types of commercially available heat flux plates with varying thickness, face area, and thermal conductivity ( $\lambda_m$ ) were evaluated. Steady-state laboratory experiments at flux densities from 20 to 175 W m<sup>-2</sup> were completed in a large box filled with dry or saturated sand having  $\lambda$  of 0.36 and 2.25 W m<sup>-1</sup> K<sup>-1</sup>. A field experiment compared  $G$  measured with pairs of four plate types buried at 6 cm in a clay soil with  $G$  determined using the gradient technique. The flux plates underestimated  $G$  in the dry sand by 2.4 to 38.5% and by 13.1 to 73.2% in saturated sand while in moist clay plate performance ranged from a 6.2% overestimate to a 71.4% underestimate. Application of the correction generally improved agreement between plate estimates and independent  $G$  measurements, especially when  $\lambda > \lambda_m$ , although most plate estimates were still significantly lower than the actual  $G$ . Limitations of the correction procedure indicate that renewed effort should be placed on innovative sensor designs that avoid or minimize heat flow distortion and/or provide direct, in situ calibration capability.

SOIL HEAT FLUX DENSITY ( $G$ ) can be measured using calorimetric, gradient, and combination techniques (Kimball and Jackson, 1979; Fuchs, 1986; Sauer, 2002), which require relatively intricate and accurate measurements of soil temperature and thermal properties. Most recent studies, however, have utilized heat flux plates (also known as heat flow meters or heat flow transducers) to measure  $G$ . Soil heat flux plates are small, rigid, disc-shaped sensors of known and constant thermal properties that are placed horizontally in the soil near the surface. The heat flux through a calibrated plate is used to estimate  $G$  in the surrounding soil at the plate depth. Credit for adapting the flux plate technique to measure heat transfer in soils is given to Falckenberg (1930). Dunkle (1940), Deacon (1950), Portman, (1958), Philip (1961), Fuchs and Tanner (1968), and Mogensen (1970) made significant contributions to the theory and design of soil heat flux plates.

Several potentially significant errors can occur when

using flux plates to measure  $G$ , including (i) heat flow distortion near the plate, (ii) liquid water and vapor flow divergence, and (iii) underestimates of  $G$  because of poor thermal contact between the plate and soil matrix (Philip, 1961; Fuchs and Hadas, 1973; Mayocchi and Bristow, 1995). Heat flow distortion near flux plates occurs because the plate is constructed of materials with fixed thermal conductivity ( $\lambda$ ) under ambient conditions while soil  $\lambda$  is influenced by mineral type, particle size and arrangement, organic matter content, bulk density, and especially soil water content (de Vries, 1963; Farouki, 1986; Bristow, 2002). Soil  $\lambda$  may range from 0.2 to 1.6 W m<sup>-1</sup> K<sup>-1</sup> with varying water content in mineral soils (Bristow, 2002). Philip (1961), in a theoretical extension of the study by Portman (1958), recommended several considerations for flux plate design to minimize heat flow distortion. Mogensen (1970) tested Philip's analysis and presented a more generalized form of Philip's equation that describes the ratio between heat flow through the meter of known dimensions and  $\lambda$  to that in the soil:

$$G_m/G = 1/[1 - \alpha r(1 - \lambda/\lambda_m)] \quad [1]$$

where  $G_m$  is the heat flux density through the plate (W m<sup>-2</sup>),  $\alpha$  is an empirical factor related to plate shape,  $r$  is a dimensionless factor equal to plate thickness divided by the square root of the area of the plate facing heat flow, and  $\lambda_m$  is the thermal conductivity of the plate. If  $\lambda$ ,  $\lambda_m$ , the plate dimensions, and  $G_m$  are known, Eq. [1] can be used to obtain a more accurate estimate of the actual soil  $G$ .

Several studies compared the performance of different flux plate designs under laboratory and/or field conditions and the utility of the correction described by Eq. [1] (Mogensen, 1970; Fuchs and Hadas, 1973; Howell and Tolk, 1990; Watts et al., 1990; van Loon et al., 1998). None of these studies were able to demonstrate a universal application of Eq. [1] that accurately corrects  $G_m$  measured with plates of differing dimensions and  $\lambda_m$ . The increasing frequency of  $G$  measurements in general and popularity of the flux plate method in particular have led to the availability of several commercial models of flux plates with widely varying dimensions and  $\lambda_m$ . The objectives of this research were to quantify heat flow distortion errors for soil heat flux plates of widely contrasting designs and to evaluate the accuracy of the previously reported correction of Philip (1961).

## MATERIALS AND METHODS

### Theory

Carslaw and Jaeger (1959, p. 427) present a solution to Laplace's equation for steady-state heat conduction in an ellipsoid (oblate spheroid) with a known thermal conductivity em-

T.J. Sauer and D.W. Meek, USDA-ARS, National Soil Tilth Laboratory, 2150 Pammel Dr., Ames, IA 50011-4420; T.E. Ochsner, USDA-ARS, Soil and Water Management Research Unit, St. Paul, MN 55108; A.R. Harris, Dep. of Physics and Astronomy, Drake University, Des Moines, IA 50311; and R. Horton, Dep. of Agronomy, Iowa State University, Ames, IA 50011. Received 13 Mar. 2003. Special Section—Advances in Measurement and Monitoring Methods. \*Corresponding author (sauer@nsl.gov).

bedded in an infinite region having a different thermal conductivity. Philip (1961) assumed that the oblate spheroid approximated the shape of a heat flux plate and derived from this solution the relationship (Philip's notation):

$$f = \frac{\varepsilon}{1 + (\varepsilon - 1) \left[ \frac{1}{1 - \eta^2} - \frac{\eta}{(1 - \eta^2)^{3/2}} \tan^{-1} \frac{(1 - \eta^2)^{1/2}}{\eta} \right]} \quad [2]$$

where  $f = G_m/G$ ,  $\varepsilon = \lambda_m/\lambda$ , and  $\eta$  is the ratio of the length of the minor to major axes of the oblate spheroid. The bracketed term in the denominator is a function of plate geometry only and was denoted  $H$ , for which Philip provides a full solution. Philip then simplified this relationship by assuming that, if  $\eta$  is "small,"  $H$  can be adequately approximated by a single-term power series expansion:

$$H(\eta) = 1 - (\pi/2)\eta \quad [3]$$

Philip then suggested that an appropriate dimensionless representation of the plate geometry would be

$$r = T/A^{1/2} \quad [4]$$

where  $T$  is the plate thickness and  $A$  is the plate face area. For the oblate spheroid,

$$r = (8/3\pi)^{1/2}\eta \quad [5]$$

which, after substitution into the expression for  $H$  reduces to

$$H = 1 - 1.70r \quad [6]$$

For a thin square plate of side length  $L$ , combining Eq. [2] and [6] leads to the following:

$$f = \frac{1}{1 - 1.70 \frac{T}{L} (1 - \varepsilon^{-1})} \quad [7]$$

and, for a thin circular plate of diameter  $D$ :

$$f = \frac{1}{1 - 1.92 \frac{T}{D} (1 - \varepsilon^{-1})} \quad [8]$$

Mogensen (1970) rearranged and generalized Eq. [7] and [8] for different plate geometries to develop the equation presented here as Eq. [1]. The values of  $\alpha$  in Eq. [7] and [8] (1.70 and 1.92) were derived by Philip (1961) but have been the source of some disagreement. Philip (1961) also calculated a square plate  $\alpha$  of 1.31 from Portman's (1958) data, noting that it was "a somewhat open question which of the values 1.31 or 1.70 is to be preferred" and further that "the discrepancy is perhaps rather trivial" (p. 573). Mogensen (1970) and Howell and Tolk (1990) reported measured  $\alpha$  values consistently lower than the calculated values, ranging from 0.89 to 1.07. Smaller  $\alpha$  values would reduce  $G_m/G$  estimates from Eq. [1], effectively improving the apparent agreement between measured and predicted plate performance for plates that underestimate  $G$ .

### Laboratory Experiment

Laboratory measurements were completed in a large box consisting of a well-insulated 46 by 51 by 8.9 cm cavity filled with dry or saturated sand in which known one-dimensional heat flux densities were established. The sand was in direct contact with a heat source plate on the bottom and heat sink

plate on top (both 1.27-cm-thick anodized aluminum). The heat source plate had four heater windings distributed in grooves on the underside of the plate through which current was applied to develop a uniform plate temperature and the desired temperature gradient through the sand. The heat sink plate had cooling fins attached to the top to promote heat dissipation. Both source and sink plates had five 0.254-mm-diameter type E (chromel/constantan) thermocouples distributed in grooves on the outer sides of the plates to monitor plate temperature. The cavity was insulated on all four sides with 10-cm-thick polystyrene insulation surrounded by 1.9-cm-thick plywood to facilitate one-dimensional heat flow between the source and sink plates.

Triplicate heat flux plates of six different types were evaluated. The plates had thicknesses from 2.6 to 7 mm, face areas from 4.9 to 27 cm<sup>2</sup>, and  $\lambda_m$  ranging from 0.26 to 1.22 W m<sup>-1</sup> K<sup>-1</sup> (Table 1). Plate  $\lambda$  values listed are those supplied by the manufacturers, which were either estimated for the primary plate material or measured in controlled laboratory settings. Laboratory measurements were performed for 7 d at each flux density of ~20, 40, 85, and 175 W m<sup>-2</sup>, first with dry sand and then with the same sand after saturation with distilled water. The sand was saturated by slowly introducing water into the bottom of one corner of the cavity to minimize air entrapment within the sand during wetting. The cavity was not large enough to accommodate all plates simultaneously. Thus, three separate experimental runs were completed: (i) CN3, GHT-1C, HFT1.1, and 610 plates; (ii) HFP01SC plates; and (iii) HFT3.1 plates. The HFP01SC plates, which have a thin film heater to enable in situ calibration, were used in passive mode in this study. Each run was completed using identical procedures. At the beginning of an experimental run, sand was added to the cavity in thin layers, leveled with a concrete float, and packed in place by tapping the side of the box. The plates were placed in the sand when the midpoint (4.5 cm above the source plate) was reached, after which sand was added until the cavity was filled. The sand used was commercial grade quartz sand composed of 20.5, 68.9, 10.2, and 0.4% coarse, medium, fine, and very fine sand (USDA classification system). Bulk density of the sand after packing the cavity was 1.75 Mg m<sup>-3</sup>.

Thermocouples (0.254-mm diam. copper/constantan) were placed in the center of the cavity 1.5, 3, 4.5, 6, and 7.5 cm above the source plate to measure the temperature profile within the sand. Two line-source  $\lambda$  probes (TC1, SoilTronics, Burlington, WA) were installed during the first experimental run to measure the sand  $\lambda$  (Bristow, 2002). Thermal conductivity measurements were completed every 4 h, and sensor signals were recorded on a datalogger (21X, Campbell Scientific, Inc., Logan, UT). Thermal conductivities measured with the line-source probes for the dry and saturated sand were 0.36 and 2.25 W m<sup>-1</sup> K<sup>-1</sup>. These values were very close to the values of  $0.33 \pm 0.01$  and  $2.18 \pm 0.12$  W m<sup>-1</sup> K<sup>-1</sup> (means  $\pm$  SD for all runs) determined using Fourier's Law:

$$G = -\lambda \partial T / \partial z \quad [9]$$

where  $\partial T / \partial z$  is the temperature gradient (K m<sup>-1</sup>) across the sand layer as measured by the source and sink plate temperatures and  $G$  was the known heat flux density through the sand.

All flux plate and thermocouple signals were recorded at 1-min intervals using solid-state thermocouple multiplexers (AM25T, Campbell Scientific) and 21X dataloggers. Hourly averages of the raw data were computed and stored for analysis. After thermal equilibration was reached during each run (~48 h), data from one continuous 24-h period were selected for analysis. Mean data from each set of three plates for each flux density were regressed against the known sand  $G$  using

**Table 1. Specifications of soil heat flux plates.**

| Model†   | Material(s)               | Shape       | Dimensions | Thickness | Thermal conductivity              |
|----------|---------------------------|-------------|------------|-----------|-----------------------------------|
|          |                           |             |            | mm        | W m <sup>-1</sup> K <sup>-1</sup> |
| CN3‡     | phenolic, stainless steel | rectangular | 48 by 29   | 7         | 0.4                               |
| HFP01SC§ | plastic, ceramic          | circular    | 80         | 5         | 0.8                               |
| GHT-1C¶  | epoxy, glass/aluminum     | square      | 52 by 52   | 5.7       | 0.26                              |
| HFT1.1#  | epoxy                     | circular    | 38         | 3.9       | 1.0                               |
| HFT3.1#  | epoxy                     | circular    | 38         | 3.9       | 1.22                              |
| 610††    | glass/epoxy               | circular    | 25         | 2.6       | 0.33                              |

† Names are necessary to report factually on available data; however, the USDA neither guarantees nor warrants the standard of the product, and the use of the name by USDA implies no approval of the product to the exclusion of others that may also be suitable.

‡ Carter-Scott Manufacturing Pty. Ltd., Brunswick, Victoria, Australia.

§ Hukseflux Thermal Sensors, Delft, The Netherlands.

¶ International Thermal Instrument Co., Del Mar, CA.

# Radiation and Energy Balance Systems, Seattle, WA.

†† C.W. Thornthwaite Associates, Pitts Grove, NJ.

weighted ordinary least squares regressions. Confidence intervals (95%) about the regression slope estimates were determined to test whether plate  $G_m$  values were significantly different from the known sand  $G$ .

### Field Experiment

Pairs of four types of flux plates (GHT-1C, 610, CN3, and HFT1.1) were installed at 6 cm in a bare clay soil near Ames, IA in the summer of 2001. The soil at this site is mapped as Canisteo series (fine-loamy, mixed, superactive, calcareous, mesic Typic Endoaquolls) and had a particle size distribution of 32% sand, 25% silt, and 43% clay. The flux plates were installed in random order at 20-cm spacing along a north-south transect. Plate installation was accomplished by excavating a shallow trench, creating small slits in one sidewall just smaller than the plate dimensions, and then inserting the plate into the slit and backfilling the trench. Soil temperature profiles were measured at two locations in the transect using thermocouples (0.511-mm diam. copper/constantan) at depths of 2, 4, 6, 9, 12, 15, 20, and 25 cm. Duplicate three-needle heat pulse sensors (Ren et al., 1999; Ochsner et al., 2001) were used to measure soil  $\lambda$  at 6 cm. The single point method of Bristow et al. (1994) was used to calculate the soil  $\lambda$  from the heat pulse sensor data. Flux plate, thermocouple, and three-needle probe signals were recorded on Campbell Scientific CR10X and 21X dataloggers, and hourly averages computed for 4 wk beginning on 3 July 2001.

Hourly soil temperature profiles from the 2- to 15-cm depths were fit with second-order polynomials, which were differentiated to obtain the temperature gradient at 6 cm. The hourly  $\lambda$  values were combined with the hourly temperature gradients to obtain  $G$  by the gradient method (Eq. [9]). Soil water content was measured by collecting five 1.9-cm-diam. soil cores several days each week. The cores were composited by depth increment and dried at 105°C for 24 h. A soil bulk density of 1.13 Mg m<sup>-3</sup> was determined from three 7.6-cm-diam., 7.6-cm-long cores collected at the outset of the experiment.

## RESULTS

### Laboratory Experiment

Performance of a particular plate design is a function of the difference between  $\lambda_m$  and  $\lambda$  and the plate geometry represented by  $r$  in Eq. [1]. The predicted  $G_m/G$  for each of the plate designs used in this study for soil  $\lambda$  from 0.2 to 2.4 W m<sup>-1</sup> K<sup>-1</sup> shows that errors in  $G$  estimates can

be as large as -55% at  $\lambda \gg \lambda_m$  (Fig. 1). There is a distinct contrast in the trend in  $G_m/G$  between the three plate types with  $\lambda_m \leq 0.4$  W m<sup>-1</sup> K<sup>-1</sup> (GHT-1C, 610, and CN3) and those with  $\lambda_m \geq 0.8$  (HFP01SC, HFT1.1, and HFT3.1). Values of  $G_m/G$  for the plates with  $\lambda_m \geq 0.8$  are generally within 20% of unity and approach a linear change with changing  $\lambda$ . The  $G_m/G$  curves for the plates with  $\lambda_m \leq 0.4$  are curvilinear with more extreme values at both low and high  $\lambda$ .

As illustrated in Fig. 1, the three flux plates with  $\lambda_m \leq 0.4$  W m<sup>-1</sup> K<sup>-1</sup> (GHT-1C, 610, and CN3) would be expected to give relatively accurate estimates of  $G$  in dry sand having  $\lambda = 0.36$ . However, results for the dry sand tests indicate that each of these plates significantly underestimated  $G$  by an average of 16.6 to 38.5% over all flux densities (Fig. 2). Contrary to Fig. 1,  $G_m$  values for the flux plates with  $\lambda_m \geq 0.8$  (HFP01SC, HFT1.1, and HFT3.1) all averaged slightly less (3.5, 8.6, and 2.4%, respectively) than the sand  $G$ . For the dry sand experiments; only the HFP01SC and HFT3.1 plate  $G_m$  regression slope estimates bounded 1 within a 95% confidence interval. The slope of all other plate  $G_m$  regressions were significantly less than 1. The slope estimates of the regression equations ranged from 0.61 (610 plate) to 0.98 (HFT3.1 plate), with  $R^2$  values all >0.999. As the saturated sand had a  $\lambda$  1.8 to 8.6 times greater than the flux plate  $\lambda_m$  values, values of  $G_m$  for all plates were expected to be significantly lower than the saturated sand  $G$ . The data are in agreement with this expectation, as average values of  $G_m$  ranged from 13.1% (HFT1.1 plate) to 73.2% (610 plate) lower than the sand  $G$  (Fig. 2). None of the 95% confidence intervals for the  $G_m$  regression slope estimates bounded 1, indicating that no plate produced a statistically accurate estimate of the saturated sand  $G$ . Regression slope estimates for the plates in saturated sand ranged from 0.27 (610 plate) to 0.88 (HFT1.1), with  $R^2$  values all >0.99.

A comparison of predicted (Eq. [1]) and measured  $G_m/G$  in dry sand showed that the measured  $G_m/G$  values were consistently lower than predicted, varying from 9.9% lower for the HFP01SC plate to 37.4% for the 610 plate (Table 2). The HFP01SC plate has a comparatively greater  $\lambda_m$  and smaller  $r$  (a small  $r$  implies less distortion of heat flow) than the 610 plate, which had a smaller  $\lambda_m$  and larger  $r$ . For the plates with  $\lambda_m \geq 0.8$ , the lower than predicted  $G_m/G$  may be attributed to poor thermal

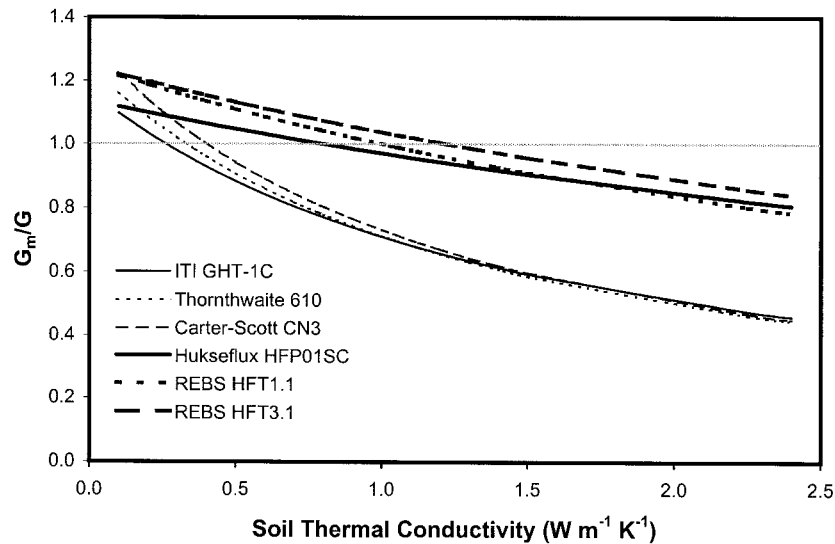


Fig. 1. Predicted ratio of heat flux density through each plate to that through the soil ( $G_m/G$ ) at varying soil  $\lambda$  determined from Eq. [1].

contact between the dry sand and the plate surfaces. Fuchs and Hadas (1973) discussed the effects of thermal contact resistance on flux plate performance, noting that contact resistance would increase with increasing particle size. Thus, it is possible that a significant contact resistance occurred during the laboratory experiments with this medium sand. For the saturated sand, measured  $G_m/G$  values were within 10% of the predicted values for each of the plates with  $\lambda_m \geq 0.8$ ; however, large differences were observed for the other three plates (Table 2). For two plates (GHT-1C and CN3), the measured  $G_m/G$  values were significantly greater than predicted, indicating that the plates performed much better than predicted in this high  $\lambda$  media.

Application of the heat flow divergence–convergence correction described in Eq. [1] had mixed results with regard to improving agreement between  $G_m$  and the known sand  $G$  (Fig. 3). Use of  $\alpha = 1.31$  instead of 1.70 as shown in Eq. [7] was found to provide better overall agreement between corrected and known  $G$  for the GHT-1C and CN3 plates and was used throughout the analysis. For dry sand, the Philip correction improved plate performance only for the two plates with the lowest  $\lambda_m$  (GHT-1C and 610). For each of the other plates, the correction progressively reduced the  $G_m$  estimates with increasing  $\lambda_m$  for an average reduction of 8.4%. Each of the plates with  $\lambda_m > 0.36$  was predicted to produce  $G_m > G$ , so the correction reduced instead of increased these  $G_m$ , thereby failing to improve the agreement. The average difference between  $G_m$  and  $G$  for all plates was  $-14.9\%$  without and  $-19.5\%$  with the Philip correction. The reverse was true for the saturated sand where the correction improved the average agreement between  $G_m$  and  $G$  from  $-36.3\%$  to  $+2.2\%$ . It is expected that thermal contact resistance would decrease with increasing water content as water would fill voids at the plate surface and improve heat transfer between plate and soil. Although Eq. [1] improved the performance of all six plate designs, the correction resulted in an overcompensation for the GHT-1C and CN3

plates. For example, the raw data for the GHT-1C plate were on average 40.4% lower than the saturated sand  $G$  but after applying the Philip correction, the corrected  $G_m$  values were now 25.2% greater than the sand  $G$ .

### Field Experiment

Data from Day 207 (26 July 2001) were used as an example data set from the field experiment to illustrate the performance of the different plate designs under field conditions (Fig. 4). Day 207 was a sunny day with moist soil following  $\sim 20$  mm of precipitation on Day 205. Accurate values for the soil  $\lambda$  are necessary not only for determination of  $G$  by the gradient method (Eq. [9]) but also for use in Eq. [1] to facilitate the heat divergence–convergence correction. The measured soil  $\lambda$  at 6 cm for Day 207 was  $1.13 \pm 0.06 \text{ W m}^{-1} \text{ K}^{-1}$  (mean  $\pm$  STD) at a volumetric water content ( $\theta$ ) of 0.25.

The  $G$  determined by the gradient method was consistently larger than all uncorrected plate  $G_m$  values except one of the HFT1.1 plates. In general, there was relatively poor agreement between duplicate plates, with the exception of the 610 plates, which were in close agreement although at very low values of  $G_m$ . Values of  $G_m/G$  were 0.29 to 1.02 for the two HFT1.1 plates, averaged  $\sim 0.60$  for the GHT-1C and CN3 plates, and averaged only 0.32 for the 610 plates. The Philip correction increased the  $G_m$  values for all plates and brought the metal-sheathed plates (GHT-1C and CN3) into close agreement (average  $G_m/G > 0.97$ ) with the gradient  $G$ . When comparing plate performance in the field with the laboratory results (Table 2), the 610 plate consistently exhibited the greatest difference between predicted and measured  $G_m/G$ . The metal-sheathed plates (GHT-1C and CN3) showed a progression of  $G_m/G$  ratios that increased with increasing soil  $\lambda$  from underestimates in dry sand to overestimates in wet sand with the best agreement for the Canisteo soil. The poor agreement between the two HFT1.1 plates in the field makes comparison with the laboratory data difficult, although the excellent per-

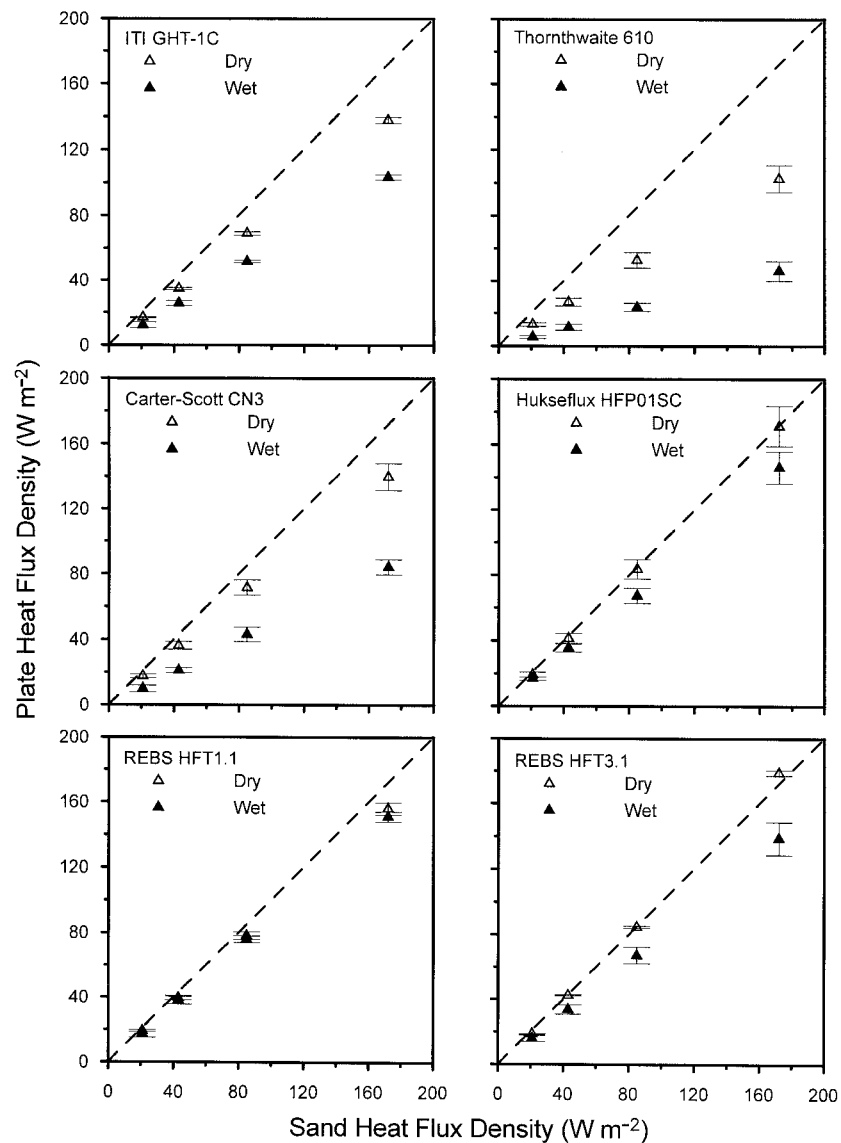


Fig. 2. Average heat flux density through each type of flux plate compared with the known flux density through the sand. Error bars represent 1 SD.

Table 2. Plate thermal conductivity ( $\lambda_m$ ), geometric shape factor from Eq. [1] ( $r$ ) and a comparison of the predicted and measured  $G_m/G$  for each plate in dry and wet (saturated) sand and in the Canisteo soil.

|                                 | GHT-1C | 610   | CN3   | HFP01SC | HFT1.1 | HFT3.1 |
|---------------------------------|--------|-------|-------|---------|--------|--------|
| $\lambda_m$ , $W m^{-1} K^{-1}$ | 0.26   | 0.33  | 0.4   | 0.8     | 1.0    | 1.22   |
| $r$                             | 0.110  | 0.117 | 0.188 | 0.071   | 0.116  | 0.116  |
| Dry sand ( $\lambda = 0.36$ )   |        |       |       |         |        |        |
| Predicted $G_m/G$               | 0.948  | 0.982 | 1.033 | 1.071   | 1.144  | 1.161  |
| Measured $G_m/G$                | 0.804  | 0.615 | 0.834 | 0.965   | 0.914  | 0.976  |
| Difference, %                   | -15.2  | -37.4 | -19.3 | -9.9    | -20.1  | -15.9  |
| Wet sand ( $\lambda = 2.25$ )   |        |       |       |         |        |        |
| Predicted $G_m/G$               | 0.476  | 0.463 | 0.404 | 0.821   | 0.802  | 0.857  |
| Measured $G_m/G$                | 0.596  | 0.268 | 0.488 | 0.818   | 0.869  | 0.783  |
| Difference, %                   | +25.2  | -42.1 | +20.8 | -0.4    | +8.4   | -8.6   |
| Canisteo ( $\lambda = 1.13$ )   |        |       |       |         |        |        |
| Predicted $G_m/G$               | 0.676  | 0.675 | 0.691 | NA†     | 0.976  | NA     |
| Measured $G_m/G$                | 0.614  | 0.322 | 0.600 | NA      | 0.674  | NA     |
| Difference, %                   | -9.2   | -52.3 | -13.2 | NA      | -30.9  | NA     |

† Not available. HFP01SC and HFT3.1 plates were not installed in the field.

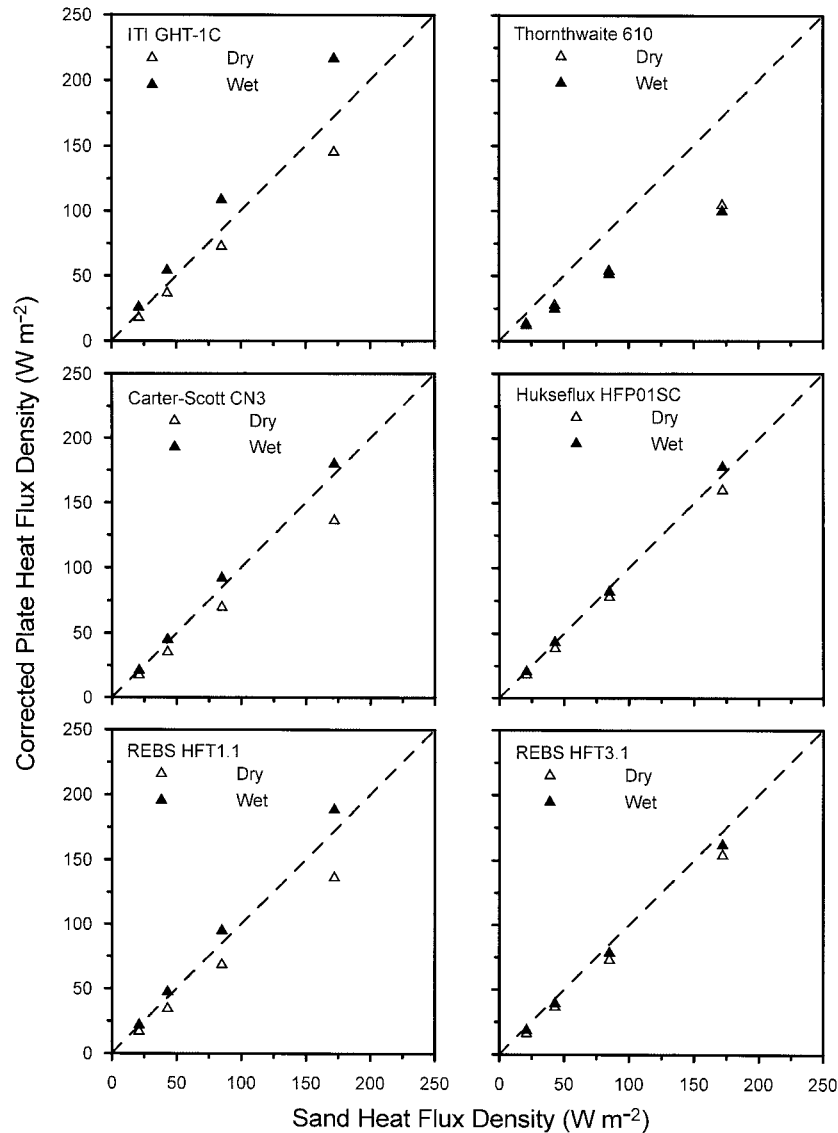


Fig. 3. Average corrected (using Eq. [1]) heat flux density through each type of flux plate compared to the known flux density through the sand.

formance of one plate ( $G_m/G = 1.02$ ) does suggest that this plate can perform very well in fine-textured soil with a  $\lambda$  similar to  $\lambda_m$ .

## DISCUSSION

Inconsistent performance of the Philip (1961) correction may be due to limitations of the theory, inability to accurately represent flux plate properties, and failure to include other factors such as contact resistance and liquid water and vapor flow divergence. The derivation of Eq. [1] is developed from a solution to Laplace's equation for steady-state heat flow in an oblate spheroid of uniform  $\lambda_m$  embedded in an infinite volume of material with different  $\lambda$  (Carslaw and Jaeger, 1959). Uncertainty in the empirical shape factor  $\alpha$  of Eq. [1] has already been discussed. Heat flux plates may not be well described by the oblate spheroid physical model as, for instance, all types tested in this study were flat with rounded edges. In most applications, there is only

a thin layer of soil above the plates, which violates the criteria of an infinite volume of media. The effect of such inconsistencies between the theory and the physical model on the accuracy of Eq. [1] are unknown and would be difficult to quantify given the scale and degree of variation in plate and soil thermal properties.

The simplified form of  $H$  described in Eq. [3] assumes that  $\eta$  is "small"; however, no criterion was given. An analysis was completed to determine whether this simplification led to significant error for the plate designs used in this study. A comparison of the full expression and single term power series approximation of  $H$  indicates a small but systematic error is introduced when the approximation is used (Fig. 5). This error ranges from 2.9% for the HFP01SC plate to 10.6% for the CN3 plate and would effectively increase the magnitude of the  $G_m$  corrections by these percentages. Nonetheless, use of the full expression for  $H$  would not significantly improve the performance of the correction.

Each flux plate design includes several materials (i.e.,

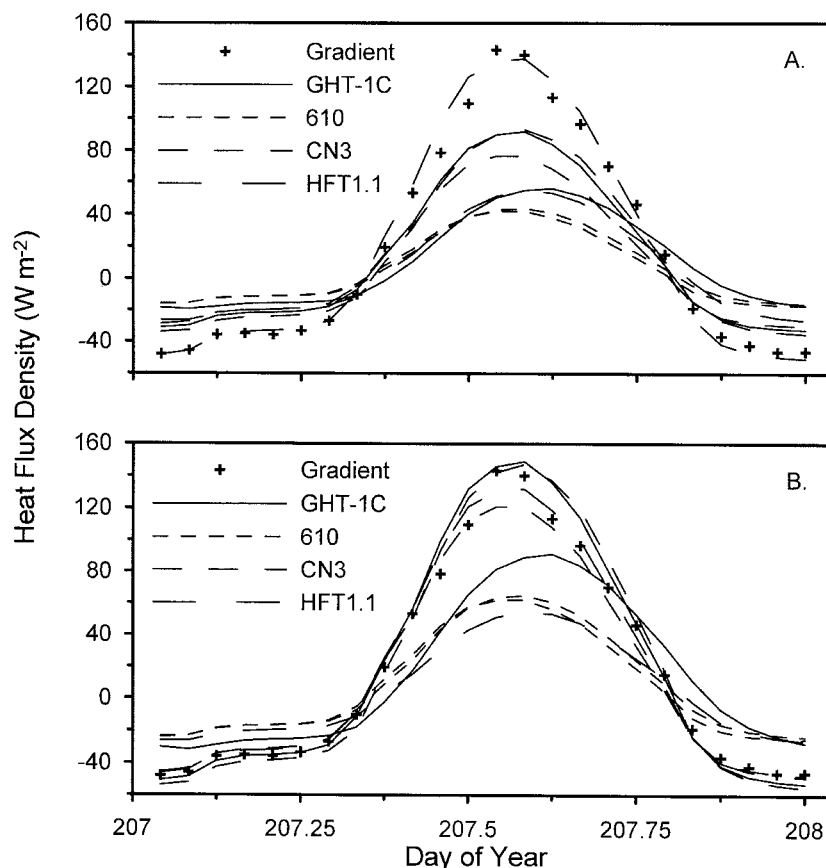


Fig. 4. (A) Uncorrected and (B) corrected  $G_m$  on Day 207 for pairs of four types of heat flux plate at 6 cm in Canisteo soil compared with  $G$  determined by Eq. [9].

epoxy, metal, glass, phenolic) that likely produce varying thermal properties across the plate body and perhaps at different depths within the plate. For instance, the HFT1.1 and HFT3.1 plates have a 204-mm<sup>2</sup> thermopile embedded in the center of the circular disk with an area of 1134 mm<sup>2</sup>. The area of the thermopile is equivalent to 18% of the plate's face area, and heat flow through this area in the center of plate is likely somewhat different than near the edges. By comparison, the HFP01SC and CN3 plate thermopile areas represent 16 and 50% of the respective plate face areas. Although any such anomalies may be compensated for during calibration procedures, there is no accommodation for nonuniform  $\lambda_m$  in the Philip correction.

Uncertainty in  $\lambda_m$  obviously impacts the ability to accurately apply Eq. [1]. Some manufacturers provide a  $\lambda_m$  that is the  $\lambda$  of the material that comprises the core or majority of the plate volume. Other manufacturers provide a measured  $\lambda_m$ ; however, there is no standard protocol for determining  $\lambda_m$ . The lack of standardized procedures for plate testing and calibration not only affects  $\lambda_m$  estimates but also introduces uncertainty regarding the accuracy of  $G_m$ . A fundamental criterion for application of the Philip (1961) procedure is that  $G_m$  is accurately known. If, for instance, the plate calibration procedure focuses on matching the thermopile signal to heat flow through the calibration media, it is not at all assured that the resulting value for  $G_m$  actually represents heat flow through the plate itself. The error in

$G_m$  would likely be least when the  $\lambda$  of the plate and calibration media are similar and contact resistance is minimal.

Philip (1961), in summarizing the limitations of his

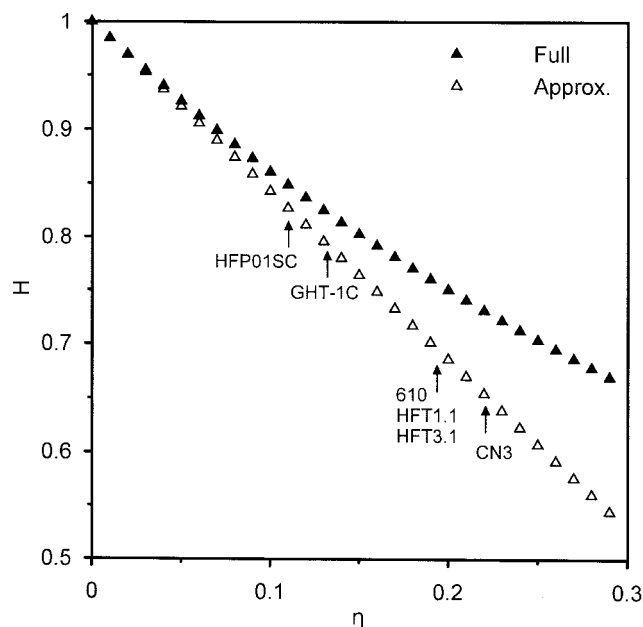


Fig. 5.  $H$  vs.  $\eta$  as defined in Eq. [2], with  $H$  determined from the full representation and from the single term of the power series approximation described in Philip (1961).

analysis of the theory of heat flux plates (meters), observed that "... uncertainties about thermal contact must set a very real limit to the accuracy of heat flux meters in media such as soils." To reduce thermal contact resistance between the flux plates and soil, Fuchs and Hadas (1973) suggested that plates be designed with high thermal conductivity metal exteriors. Two of the plate designs evaluated here had metal sheaths on the faces of the plate (GHT-1C and CN3); these were the same two plates that performed much better than predicted in saturated sand. Since contact resistance is a function of air gaps between the plate and soil, differences in soil particle size, structure, and water content would all affect contact resistance and thus plate performance. For these reasons, Fuchs and Hadas (1973) and Höglström (1974) advocated in situ calibration to assess plate performance and minimize the potentially confounding effects of varying contact resistance.

The field data set illustrates some of the difficulties in making accurate  $G$  measurements in the field and the challenges for using Eq. [1] to obtain more accurate estimates of  $G$ . Even though all eight plates were installed at the same time using the same procedure in what appeared to be a uniform soil, there was poor agreement between some pairs, in particular for the HFT1.1 and GHT-1C plates. Unlike the laboratory experiment, it is very difficult to ascertain whether differences between  $G$  measurements in the field are due to sensor performance (i.e., high thermal contact resistance), spatial variation in  $G$ , or liquid water or water vapor flow divergence. In addition,  $G$  measured by the gradient method is also subject to uncertainties. Contact resistance errors are very difficult to detect under field conditions, even if the plate is exposed for inspection. It is generally assumed that soil wetting and drying cycles improve thermal contact between plate and soil as, with time, the soil particle arrangement conforms to the surface of the plate. If uniform soil properties and  $G$  can be assumed, then three of the four plates with the Philip (1961) correction appear to have potential to produce acceptable  $G$  estimates in this structured clay soil. The 610 plates, as in the laboratory experiments, clearly significantly underestimate  $G$  and the correction fails to bring the plate  $G_m$  values into acceptable agreement with the gradient  $G$ .

Impermeable flux plates do impede the flow of liquid water and water vapor (Mayocchi and Bristow, 1995), which may include the transfer of latent heat that is not sensed by the plate. Water flow divergence may also result in a different water content and therefore  $\lambda$  in the soil immediately above and below the plate. This nonuniformity of soil  $\lambda$  could have significant effects on both flux plate performance and any attempt to apply the Philip correction. Even when accurate measurements of  $G$  are obtained at the plate depth,  $G$  at the soil surface is often desired for surface energy balance calculations. Failing to account for heat storage in the soil layer above the flux plates introduces another significant source of error in the estimate of surface  $G$  (Sauer and Horton, 2003), but even this correction is still sometimes ignored (Wilson et al., 2002).

The availability of inexpensive soil heat flux plates

and the wide use of dataloggers has led to the practice of installing one to several flux plates at a shallow depth and accepting the measured  $G$  with limited examination for potential errors. While significant progress has been made in field instrumentation used in soil thermal property and micrometeorology research, the technology behind soil heat flux plates has remained relatively unchanged for at least two decades. It is readily apparent that there is potential for significant errors in measured  $G$  associated with the use of heat flux plates including heat flow distortion, thermal contact resistance, and water flow divergence. Much greater attention to errors in  $G$  measurement is warranted and necessary to improve the accuracy of  $G$  measurements similar to the technological improvements of associated turbulent flux and soil thermal property measurements. Recent advancements in flux plate technology include the development of the HFP01SC flux plate with an internal heater element that allows an in situ calibration to the adjacent soil thermal properties. Another promising development is the design of a printed circuit flux plate that is very thin and may allow for a perforated construction that would eliminate water flow divergence (Robin et al., 1997). Such efforts are needed to continue the evolution of flux plate designs that minimize errors due to heat and water flow divergence and thermal contact resistance.

## CONCLUSIONS

Flux plate measurements of  $G$  are likely to include significant errors that are not widely identified nor frequently addressed. Each type of flux plate evaluated routinely underestimated  $G$  in both controlled laboratory experiments with sand and in a structured clay soil in the field, with errors ranging from <10% to >70%. The range of errors was in broad agreement with those predicted by the Philip analysis; however, the correction procedure was found to be useful primarily when  $\lambda > \lambda_m$  and then not for all plate types. These findings are consistent with previous research and suggest that limitations to the underlying theory, uncertainty in plate thermal properties and heat flow through the plate, contact resistance, and water flow divergence may all contribute to the observed unsatisfactory performance of the Philip correction.

Even if the limitations of the Philip analysis could be addressed, correction for heat flow distortion would require continuous measurement of soil  $\lambda$  near the plate and calculation of  $G_m/G$  as  $\lambda$  changes. This process would not be trivial for any long-term field experiment (i.e., energy balance studies), especially in humid regions with significant wetting and drying cycles in surface soil layers. Results of this study indicate that it is doubtful whether further effort to enhance the Philip (or any similar) correction is warranted. Recent advancements such as the in situ calibration capability of the HFP01SC plate may provide an integrated and direct approach for addressing heat flow distortion errors. More accurate field measurements of  $G$  will likely result if research emphasis is directed to investigating innovative new sensor designs that avoid or minimize heat flow

distortion and/or provide direct, in situ calibration capability.

### ACKNOWLEDGMENTS

Appreciation is extended to Paul Doi and Anna Myhre of the National Soil Tilth Laboratory and Bert Tanner and Ed Swiatek of Campbell Scientific, Inc. for their assistance with this study. Iowa State University Agronomy Department Endowment funds and the Program for Women in Science and Engineering provided partial support for this work.

### REFERENCES

- Bristow, K.L. 2002. Thermal conductivity. p. 1209–1226. *In* G.C. Topp and J.H. Dane (ed.) *Methods of soil analysis*. Part 4. SSSA Book Ser. 5. SSSA, Madison, WI.
- Bristow, K.L., G.J. Kluitenberg, and R. Horton. 1994. Measurement of soil thermal properties with a dual-probe heat-pulse technique. *Soil Sci. Soc. Am. J.* 58:1288–1294.
- Carslaw, H.S., and J.C. Jaeger. 1959. *Conduction of heat in solids*. 2nd ed. Clarendon Press, Oxford.
- Deacon, E.L. 1950. The measurement and recording of the heat flux into the soil. *Q. J. R. Meteorol. Soc.* 76:479–483.
- de Vries, D.A. 1963. Thermal properties of soils. p. 210–235. *In* W.R. van Wijk (ed.) *Physics of plant environment*. North-Holland Publ., Amsterdam.
- Dunkle, R.V. 1940. Heat meters. *Bull. Am. Meteorol. Soc.* 21:116–117.
- Falckenberg, G. 1930. Apparatur zur Bestimmung des momentanen nächtlichen Wärmeaustausches zwischen Erde und Luft. *Meteorol. Zeitschrift*. 47:154–156.
- Farouki, O.T. 1986. Thermal properties of soils. Series on rock and soil mechanics. Vol. 11. Trans Tech Publications, Clausthal-Zellerfeld, Germany.
- Fuchs, M. 1986. Heat flux. p. 957–968. *In* A. Klute (ed.) *Methods of soil analysis*. Part 1. 2nd ed. SSSA Book Ser. 5. SSSA, Madison, WI.
- Fuchs, M., and A. Hadas. 1973. Analysis and performance of an improved soil heat flux transducer. *Soil Sci. Soc. Am. Proc.* 37:173–175.
- Fuchs, M., and C.B. Tanner. 1968. Calibration and field test of soil heat flux plates. *Soil Sci. Soc. Am. Proc.* 32:326–328.
- Högström, U. 1974. In situ calibration of ground heat flux plates. *Agric. Meteorol.* 13:161–168.
- Howell, T.A., and J.A. Tolk. 1990. Calibration of soil heat flux transducers. *Theor. Appl. Climatol.* 42:263–272.
- Kimball, B.A., and R.D. Jackson. 1979. Soil heat flux. p. 211–229. *In* B.J. Barfield and J.F. Gerber (ed.) *Modification of the aerial environment of plants*. ASAE Monogr. 2. ASAE, St. Joseph, MI.
- Mayocchi, C.L., and K.L. Bristow. 1995. Soil surface heat flux: Some general questions and comments on measurements. *Agric. For. Meteorol.* 75:43–50.
- Mogensen, V.O. 1970. The calibration factor of heat flux meters in relation to the thermal conductivity of the surrounding medium. *Agric. Meteorol.* 7:401–410.
- Ochsner, T.E., R. Horton, and T. Ren. 2001. A new perspective on soil thermal properties. *Soil Sci. Soc. Am. J.* 65:1641–1647.
- Philip, J.R. 1961. The theory of heat flux meters. *J. Geophys. Res.* 66:571–579.
- Portman, D.J. 1958. Conductivity and length relationships in heat-flow transducer performance. *Trans. Am. Geophys. Union* 39:1089–1094.
- Ren, T., K. Noborio, and R. Horton. 1999. Measuring soil water content, electrical conductivity, and thermal properties with a thermo-time domain reflectometry probe. *Soil Sci. Soc. Am. J.* 63:450–457.
- Robin, P., P. Cellier, and G. Richard. 1997. Theoretical and field comparison of two types of soil heat fluxmeter. *Soil Technol.* 10:185–206.
- Sauer, T.J. 2002. Heat flux density. p. 1233–1248. *In* G.C. Topp and J.H. Dane (ed.) *Methods of soil analysis*. Part 4. SSSA Book Ser. 5. SSSA, Madison, WI.
- Sauer, T.J., and R. Horton. 2003. Soil heat flux. *In* J.L. Hatfield and J.H. Baker (ed.) *Micrometeorological measurements in agricultural systems*. ASA Monograph. American Society of Agronomy, Madison, WI. In press.
- van Loon, W.K.P., H.M.H. Bastings, and E.J. Moors. 1998. Calibration of soil heat flux sensors. *Agric. For. Meteorol.* 92:1–8.
- Watts, D.B., E.T. Kanemasu, and C.B. Tanner. 1990. Modified heat-meter method for determining soil heat flux. *Agric. For. Meteorol.* 49:311–330.
- Wilson, K., A. Goldstein, E. Falge, M. Aubinet, D. Baldocchi, P. Bergigier, C. Bernhofer, R. Ceulemans, H. Dolman, C. Field, A. Grelle, A. Ibrom, B.E. Law, A. Kowalski, T. Meyers, J. Moncrieff, R. Monson, W. Oechel, T. Tenhunen, R. Valentini, and S. Verma. 2002. Energy balance closure at FLUXNET sites. *Agric. For. Meteorol.* 113:223–243.